Contrast-enhanced Dedicated Breast CT: Initial Clinical Experience[1]

Nicolas D. Prionas, MS
Karen K. Lindfors, MD
Shonket Ray, MS
Shih-Ying Huang, BS
Laurel A. Beckett, PhD
Wayne L. Monsky, MD, PhD
John M. Boone, PhD

Purpose: To quantify contrast material enhancement of breast lesions scanned with dedicated breast computed tomography (CT) and to compare their conspicuity with that at unenhanced breast CT and mammography.

Materials and Methods: Approval of the institutional review board and the Radiation Use Committee and written informed consent were obtained for this HIPAA-compliant study. Between September 2006 and April 2009, 46 women (mean age, 53.2 years; age range, 35–72 years) with Breast Imaging Reporting and Data System category 4 or 5 lesions underwent unenhanced breast CT and contrast material–enhanced breast CT before biopsy. Two radiologists independently scored lesion conspicuity for contrast-enhanced breast CT versus mammography and for contrast-enhanced breast CT versus unenhanced breast CT. Mean lesion voxel intensity was measured in Hounsfield units and normalized to adipose tissue intensity on manually segmented images obtained before and after administration of contrast material. Regression models focused on conspicuity and quantified enhancement were used to estimate the effect of pathologic diagnosis (benign vs malignant), lesion type (mass vs calcifications), breast density, and interradiologist variability.

Results: Fifty-four lesions (25 benign, 29 malignant) in 46 subjects were analyzed. Malignant lesions were seen significantly better at contrast-enhanced breast CT than at unenhanced breast CT ($P < .001$) or mammography ($P < .001$). Malignant calcifications (malignant lesions manifested mammographically as microcalcifications only, $n = 7$) were seen better at contrast-enhanced breast CT than at unenhanced breast CT ($P < .001$) and were seen similarly at contrast-enhanced breast CT and mammography. Malignant lesions enhanced 55.9 HU ± 4.0 (standard error), whereas benign lesions enhanced 17.6 HU ± 6.1 ($P < .001$). Ductal carcinoma in situ ($n = 5$) enhanced a mean of 59.6 HU ± 2.8. Receiver operating characteristic curve analysis of lesion enhancement yielded an area under the receiver operating characteristic curve of 0.876.

Conclusion: Conspicuity of malignant breast lesions, including ductal carcinoma in situ, is significantly improved at contrast-enhanced breast CT. Quantifying lesion enhancement may aid in the detection and diagnosis of breast cancer.

[1] From the Department of Radiology, University of California Davis Medical Center, 4860 Y St, Suite 3100, Sacramento, CA 95817 (N.D.P., K.K.L., S.R., S.Y.H., W.L.M., J.M.B.); and Division of Biostatistics, Department of Public Health Sciences, University of California Davis, Davis, Calif (L.A.B.). From the 2009 RSNA Annual Meeting. Received December 8, 2009; revision requested February 3, 2010; final revision received February 23; accepted March 18; final version accepted March 30. L.A.B. supported by a Biostatistics Shared Resource of the University of California Davis Cancer Center Support Grant (P30CA093373-06). **Address correspondence to** K.K.L. (e-mail: *kklindfors@ucdavis.edu*).

Dedicated breast computed tomography (CT) is an emerging technology that may improve the early detection of breast cancer, a disease that takes the lives of more than 40 000 women a year (1). Although mammography is the current standard for breast cancer screening, it has the drawback of the superimposition effects found in projection imaging, where overlying normal breast tissue can obscure a lesion, thereby hindering detection, or it can cause summation artifacts leading to false-positive results, recalls, and additional studies. As a fully tomographic modality, breast CT may improve the detection and diagnosis of breast cancer. In an initial clinical study, there was no significant difference between breast CT and mammography in distinguishing benign from malignant lesions (2). Unenhanced breast CT was superior to mammography in the visualization of breast masses. However, mammography outperformed breast CT in the visualization of microcalcifications. For dedicated breast CT to succeed as a screening modality in the early detection of breast cancer, its sensitivity and specificity, especially for detection of ductal carcinoma in situ (DCIS), must be improved over the sensitivity and specificity of mammography.

Other breast imaging modalities, including dynamic contrast material–enhanced magnetic resonance (MR) imaging and other investigational methods, have involved injection of contrast material to improve lesion conspicuity (3–7). Since the Hounsfield unit in CT is linearly proportional to attenuation, contrast-enhanced CT with a nonionic, iodine-based contrast medium may be a useful tool for quantification of the differential capillary permeability between normal and malignant tissues (8–11). Although investigators in previous studies explored breast cancer detection with contrast-enhanced multidetector whole-body CT (5) and single-section dedicated breast CT (12–14), the usefulness of contrast material enhancement in dedicated cone-beam breast CT has not, to our knowledge, been studied. Our aim was to quantify contrast material enhancement of breast lesions scanned with dedicated breast CT and to compare their conspicuity with that at unenhanced breast CT and mammography.

Advances in Knowledge

- Malignant mass lesions are significantly more conspicuous than benign lesions at contrast-enhanced dedicated breast CT when compared with mammography and unenhanced breast CT ($P < .001$ for each comparison).
- Visualization of malignant calcifications (malignant lesions manifested mammographically as microcalcifications only) at contrast-enhanced breast CT is improved over that at unenhanced breast CT ($P < .001$) and is similar to that at mammography ($P = .64$).
- Malignant breast lesions enhance by a mean of 38 HU more than do benign lesions ($P < .001$), and receiver operating characteristic curve analysis yields an area under the receiver operating characteristic curve of 0.876.

Materials and Methods

One author (J.M.B.) is a consultant to Varian Imaging Systems (Palo Alto, Calif) and Artemis (Erlangen, Germany) and receives funding from Varian Imaging Systems, Fuji Medical Systems (Stamford, Conn), and Hologic (Bedford, Mass). Several of these relationships may pertain to the ultimate commercialization of breast CT and related topics. In addition, this author has a patent pending on various breast CT topics. All other authors had control of all data that may have presented a conflict of interest.

Implications for Patient Care

- The use of intravenous contrast material with breast CT improves visualization of malignant lesions, including ductal carcinoma in situ.
- Contrast-enhanced breast CT has potential as a qualitative and quantitative imaging modality in breast cancer screening and diagnosis.

Subject Selection

Women with mammographically or ultrasonographically (US) identified Breast Imaging Reporting and Data System (BI-RADS) category 4 or 5 lesions were recruited sequentially between September 2006 and April 2009 for contrast-enhanced breast CT. One subject was reported previously in a preliminary study of unenhanced breast CT (2). Subjects were recruited by four mammographers in our department, two of whom also evaluated the breast CT images (K.K.L.). Subject recruitment and subject studies were performed in accordance with protocols approved by our institutional review board, including approval from the Radiation Use Committee and the Cancer Center Scientific Review Committee. Written informed consent was obtained, and Health Insurance Portability and Accountability Act guidelines were observed. Subjects with renal dysfunction or other contraindications to contrast material were excluded from the study. In total, 46 women (mean age, 53.2 years; age range, 35–72 years)

Published online
10.1148/radiol.10092311

Radiology 2010; 256:714–723

Abbreviations:
BI-RADS = Breast Imaging Reporting and Data System
DCIS = ductal carcinoma in situ

Author contributions:
Guarantors of integrity of entire study, N.D.P., K.K.L., S.R.; study concepts/study design or data acquisition or data analysis/interpretation, all authors; manuscript drafting or manuscript revision for important intellectual content, all authors; manuscript final version approval, all authors; literature research, N.D.P., K.K.L., S.Y.H., W.L.M.; clinical studies, N.D.P., K.K.L., S.Y.H., W.L.M.; statistical analysis, N.D.P., K.K.L., S.Y.H., L.A.B.; and manuscript editing, N.D.P., K.K.L., S.Y.H., L.A.B., W.L.M., J.M.B.

Funding:
This research was supported by the National Institutes of Health (grants R01 EB002138 and UL1 RR024146).

See Materials and Methods for pertinent disclosures.

underwent contrast-enhanced breast CT followed immediately by image-guided biopsy. Only histologically diagnosed lesions were included in the study.

Breast density was characterized at mammography according to BI-RADS criteria as fatty (<25% dense), scattered fibroglandular density (25%–50% dense), heterogeneously dense (51%–75% dense), or extremely dense (>75% dense). For regression analyses, each density group was quantitatively categorized with a score of 1, 2, 3, or 4. Because of the small sample sizes in each density category, breasts with a density score of 1 or 2 were grouped as low density and breasts with a score of 3 or 4 were grouped as high density.

Image Acquisition

Each subject underwent contrast-enhanced breast CT with a previously described dedicated cone-beam breast CT system (15). The breast CT technique factors were set to a tube voltage of 80 kVp, and tube current was adjusted for each subject according to breast size and mammographic density, such that each scan delivered a mean glandular radiation dose equivalent to that of two-view screening mammography (4–16 mGy) (16). A complete contrast-enhanced breast CT series included a total of four approximately 17-second breast CT scans imaging one breast at a time before and after contrast material injection so that the total radiation dose to each breast (8–32 mGy) was twice that of a single unenhanced breast CT scan. Scanning of the unaffected breast was performed first (before administration of contrast material) and was followed by precontrast scanning of the affected breast (containing the index lesion). Thereafter, scanning of the affected breast was performed after administration of contrast material. Finally, postcontrast scanning of the unaffected breast was performed. In this way, delay after contrast material injection was controlled in scanning the affected breast, and repositioning of the affected breast was minimized. One hundred milliliters of intravenous iodixanol (Visipaque 320; GE Healthcare, Waukesha, Wis) was administered at a rate of 4 mL/sec with a power injector. The injection protocol was adapted from the protocol used in multiphase abdominal studies at our institution. The average delay from the start of contrast material injection until postcontrast scanning was 96 seconds (range, 52–219 seconds for ipsilateral lesions, 247 seconds for the single contralateral lesion). Contrast material delay time was derived empirically.

Lesion Conspicuity Analysis

The conspicuity of lesions at mammography (46 digital and eight screen-film mammograms, including craniocaudal and mediolateral oblique views only, were obtained), breast CT, and contrast-enhanced breast CT was compared subjectively and independently in sequential order by two radiologists (K.K.L.), both of whom had more than 15 years of experience in breast imaging and at least 2 years of experience with dedicated breast CT. No other images from diagnostic imaging studies were included in the comparison. The reviewing radiologist had access to both studies (contrast-enhanced breast CT images and either mammograms or unenhanced breast CT images) at the same time but did not have knowledge of histologic findings. Contrast-enhanced CT images were evaluated first. If the lesion was not readily identified on the contrast-enhanced CT images, the images from the comparison modality (mammography or unenhanced breast CT) were examined and, with the knowledge from that evaluation, the contrast-enhanced CT images were reinterpreted for the comparison. Conspicuity was evaluated by comparing *(a)* contrast-enhanced breast CT with mammography and *(b)* contrast-enhanced breast CT with unenhanced breast CT. The differential conspicuity of each lesion between modalities was scored by using a continuous scale from 1 to 10, allowing half points, where 1 indicated excellent conspicuity at contrast-enhanced breast CT and poor conspicuity with the comparison modality, 10 indicated excellent conspicuity with the comparison modality (mammography or unenhanced breast CT) and poor conspicuity at contrast-enhanced breast CT, and 5.5 indicated equivalent conspicuity with both modalities.

Quantitative Image Analysis

Images were analyzed by using a graphical user interface (Matlab 7.0 with Image Processing Toolbox 4.2; MathWorks, Natick, Mass). Each lesion was segmented from the pre- and postcontrast breast CT images by manually outlining the region of interest in every section containing the lesion. Segmentation was performed by three authors (N.D.P., primarily precontrast images; S.R., primarily postcontrast images; and S.Y.H., random subset of images) with 4, 5, and 5 years of experience with dedicated breast CT, respectively. Descriptive statistics, including mean voxel intensity in Hounsfield units ± standard deviation, were calculated for the volume of interest. More than 5500 regions of interest were segmented manually with constant window (350 HU) and level (25 HU) settings. Five rectangular regions of interest (mean area, 3758 pixels; range, 258–19 170 pixels) outlining only adipose tissue were drawn within the image sets of each breast volume. Mean adipose tissue intensity was used to normalize lesion intensity and account for any fluctuations between image acquisitions. Lesion enhancement was calculated as the difference between normalized lesion intensity in the pre- and postcontrast image sets with the following equation:

$$\Delta HU = \left(HU_L^{Post} - HU_A^{Post}\right) - \left(HU_L^{Pre} - HU_A^{Pre}\right),$$

where L and A represent the lesion intensity and adipose tissue intensity, respectively, measured in the precontrast (Pre) and postcontrast (Post) image sets.

Quantitative analysis was performed in 52 lesions. Seven of the benign lesions were identified initially by means of US or mammography but were not identifiable at unenhanced breast CT or contrast-enhanced breast CT (no enhancement). The seven cases (three fibrocystic changes, one cyst, one stromal fibrosis, one unremarkable fibroadipose

tissue, and one adenosis and fibrosis with microcalcifications) were identified as calcifications ($n = 4$), had negative mammographic findings ($n = 2$), or were identified as a mass ($n = 1$). In these cases, average glandular tissue intensity of the entire breast was calculated from segmented unenhanced breast CT and contrast-enhanced breast CT images and used as a surrogate for lesion intensity. Two mammographically identified lesions were not identified at unenhanced breast CT or contrast-enhanced breast CT and were present in breasts containing another identified malignant lesion. As a result, overall mean glandular tissue intensity could not be used as a surrogate for lesion intensity. Both lesions were benign (focal fibrosis and fibrocystic change) and were excluded from the quantitative analysis.

Statistical Analyses

Lesion conspicuity scores were adjusted by subtracting 5.5, so that a score of zero corresponded to equivalent conspicuity between modalities, negative values corresponded to better conspicuity at contrast-enhanced breast CT, and positive values corresponded to better conspicuity with the comparison modality (mammography or unenhanced breast CT). We began by calculating univariate statistical summaries (mean ± standard deviation) of the scores for each comparison. Standard error estimates for the mean score were examined by using paired t tests, adjusted for within-subject clustering, and validated by using a Wilcoxon signed rank procedure as a complementary nonparametric approach.

Mixed-effects linear regression models were designed to compare conspicuity scores at contrast-enhanced breast CT with those at mammography and unenhanced breast CT according to lesion subgroups, taking into account pathologic diagnosis (malignant vs benign), lesion type (mass vs calcification), and interradiologist variability, adjusting for clustering from repeated observations of the same lesion and, in seven subjects, multiple lesions per subject. In univariate models, we examined whether breast density played a role in lesion conspicuity.

Quantitative benign and malignant lesion enhancements were compared initially by using a two-sample Wilcoxon rank sum test. Subgroup analysis according to pathologic diagnoses was performed by using the Kruskal-Wallis test. We then fitted mixed-effects linear regression models estimating lesion enhancement and its relationship to pathologic diagnosis, lesion type, breast density, and delay between contrast material injection and postcontrast scanning, adjusted for clustering. Receiver operating characteristic curve analysis was performed on histograms of benign and malignant lesion enhancement.

All statistical analyses were performed by using software (SAS, version 9, SAS Institute, Cary, NC; Stata, version 11, Stata, College Station, Tex). Statistical significance was assumed when the two-sided P value was less than .05.

Results

In the 46 women, 54 lesions were identified for inclusion in the study (Table 1). Of the 54 lesions, 40 (74%) were not palpable according to referral history and were found at screening in asymptomatic women. Three (6%) of the palpable lesions had negative mammographic findings and were identified at US. One of the three mammographically occult lesions (mucinous adenocarcinoma) was identified at breast CT and contrast-enhanced breast CT. Seven subjects had multiple lesions; three of those subjects had two malignant lesions of the same histopathologic type in the same breast, and three subjects had one malignant lesion and one benign lesion in the same breast. One subject had a benign fibroadenoma in the left breast and two lesions, a fibroadenoma and a malignant lesion of mixed invasive ductal carcinoma and DCIS, in the right breast. The mean lesion volume of interest was 1615.4 mm^3 (range, 5.1–10451.4 mm^3) on the precontrast image. Average breast density was 2.78 ± 0.15 (standard error). Post hoc power analysis with power equal to 0.90 necessitated acquisition of 13 samples to detect a one-point conspicuity score difference for malignant lesions and acquisition of 21 samples to detect a 38-HU difference in lesion enhancement between malignant and benign lesions ($P < .05$).

Table 1

Pathologic Diagnoses of 54 Breast Lesions

Type of Lesion	No. of Lesions
Malignant	29
Mass	22
Invasive ductal carcinoma	10
Invasive mammary carcinoma	7
Mixed	4
Mucinous	1
Calcification	7
DCIS	5
Mixed	2
Benign	25
Mass	15
Fibroadenoma	7
Stromal fibrosis	2
Cyst	1
Other	5
Calcification	10
Fibrocystic change	7
Other	3

Note.—There was a total of 54 lesions, 37 of which were masses and 17 of which were calcifications.

Lesion Conspicuity

Malignant lesions were significantly more conspicuous at contrast-enhanced breast CT than at mammography ($P < .001$) (Table 2). The conspicuity of malignant lesions identified at mammography as microcalcifications did not differ significantly between the two modalities ($P = .64$). Benign masses were significantly more conspicuous at contrast-enhanced breast CT than at mammography ($P = .003$); however, benign calcifications were visualized significantly better at mammography than at contrast-enhanced breast CT ($P = .004$).

Mixed-effects regression models were used to compare lesion conspicuity at contrast-enhanced breast CT with that at mammography, and they enabled us to confirm the trends observed with mean conspicuity scores (Table 3). The difference in mean conspicuity scores between all malignant lesions

Table 2

Mean Conspicuity of Lesions Visualized at Contrast-enhanced Breast CT, Mammography, and Unenhanced Breast CT

		Contrast-enhanced Breast CT vs Mammography		Contrast-enhanced Breast CT vs Unenhanced Breast CT	
Group	No. of Lesions	Mean Conspicuity	*P* Value	Mean Conspicuity	*P* Value
Malignant	29	−1.45 (−1.95, −0.95)	<.001	−1.76 (−2.12, −1.4)	<.001
Mass	22	−1.84 (−2.26, −1.42)	<.001	−1.56 (−1.96, −1.16)	<.001
Calcification	7	−0.29 (−1.45, 0.87)	.64	−2.36 (−3.1, −1.62)	<.001
Benign	25	0.34 (−0.58, 1.26)	.46	−0.84 (−1.3, −0.38)	.001
Mass	15	−1.07 (−1.65, −0.49)	.003	−0.67 (−1.21, −0.13)	.03
Calcification	10	2.33 (1.13, 3.53)	.004	−1.08 (−1.86, −0.3)	.02
All lesions	54	−0.52 (−1.08, 0.04)	.07	−1.3 (−1.62, −0.98)	<.001
Mass	37	−1.47 (−1.85, −1.09)	<.001	−1.13 (−1.49, −0.77)	<.001
Calcification	17	1.25 (0.21, 2.29)	.03	−1.6 (−2.22, −0.98)	<.001

Note.—Data in parentheses are 95% confidence intervals. Negative scores correspond to better visualization at contrast-enhanced breast CT. Positive scores correspond to better conspicuity with the comparison modality (mammography or unenhanced breast CT). Scores of zero correspond to equivalent conspicuity between modalities. *P* values were calculated with the *t* test and adjusted for within-subject correlation.

Table 3

Regression-estimated Conspicuity When Comparing Contrast-enhanced Breast CT with Mammography

Parameter	Overall Mean	Mass Mean	Calcification Mean	Absolute Difference*
Overall	…	−1.60 (37)	1.51 (17)	3.11 ($P < .001$)
Benign	0.46 (25)	−0.99 (15)	2.53 (10)	3.52 ($P < .001$)
Malignant	−1.40 (29)	−1.86 (22)	−0.27 (7)	1.59 ($P = .01$)
Absolute difference†	1.86 ($P < .001$)	0.87 ($P = .01$)	2.80 ($P < .001$)	1.93 ($P = .01$)‡

Note.—Unless otherwise indicated, data in parentheses are numbers of lesions. *P* values represent the significance of the difference in mixed-effects linear regression–estimated mean conspicuity scores for the compared lesion subgroups and have been adjusted for interradiologist variation, within-subject clustering, and breast density.

* Mass versus calcification.

† Benign versus malignant.

‡ Interaction of the malignancy and lesion type (mass or calcification) factors.

versus all benign lesions, malignant masses versus benign masses, and malignant calcifications (malignant lesions manifested mammographically as microcalcifications only) versus benign calcifications was significant in all three comparisons ($P < .001$, $P = .01$, and $P < .001$, respectively), with the malignant lesions having better conspicuity at contrast-enhanced breast CT in all three comparisons.

In the comparison of contrast-enhanced breast CT and unenhanced breast CT, mean lesion conspicuity was significantly greater at contrast-enhanced breast CT for all lesion types (Table 2). Malignant lesions, including those with calcifications, were seen significantly better with contrast-enhanced breast CT ($P < .001$) (Figs 1, 2).

Regression models were used to compare lesion conspicuity at contrast-enhanced breast CT with that at unenhanced breast CT. This reinforced the fact that all lesion types were seen better at contrast-enhanced breast CT (Table 4). Mean conspicuity scores at contrast-enhanced breast CT were significantly higher for malignant lesions than for benign lesions ($P < .001$) and for malignant calcifications than for benign calcifications ($P = .01$).

In the comparison of contrast-enhanced breast CT with mammography and unenhanced breast CT, interobserver variabilities between the two radiologists were 0.13 ± 0.19 ($P = .50$) and 0.37 ± 0.18 ($P = .05$), respectively. The observer with less experience reported a larger conspicuity difference at contrast-enhanced breast CT than at unenhanced breast CT.

Effects of Breast Density on Lesion Conspicuity

High- and low-density breasts had mean conspicuity scores that favored contrast-enhanced breast CT over mammography (−0.48 and −0.58, respectively), but neither was significant ($P = .23$ and $P = .17$, respectively). Lesion conspicuity was greater at contrast-enhanced breast CT than at unenhanced breast CT for lesions found in both high-density ($P < .001$) and low-density ($P < .001$) breasts, with lesion conspicuity in high-density breasts scored even more toward contrast-enhanced breast CT (mean conspicuity, −1.45) than that in low-density breasts (mean conspicuity, −1.07). In regression models, each increasing BI-RADS density group slightly shifted conspicuity toward contrast-enhanced breast CT by 0.20 ± 0.26 ($P = .44$) and 0.21 ± 0.15 ($P = .16$) when comparing contrast-enhanced breast CT with mammography and unenhanced breast CT, respectively; however, these results were not significant.

Radiology

Quantitative Lesion Enhancement

The differential enhancement between benign (17.6 HU ± 6.1) and malignant (55.9 HU ± 4.0) lesions was significant ($P < .001$). Receiver operating characteristic curve analysis yielded an area under the receiver operating characteristic curve of 0.876 (Fig 3).

Regression models of lesion enhancement show that malignant lesions enhance more than do benign lesions ($P < .001$) (Table 5). Malignant lesions identified as calcifications enhanced 34.6 HU more than did benign lesions identified as calcifications ($P = .01$). Malignant masses enhanced significantly more than did benign masses ($P < .001$). Breast density and contrast material delay did not significantly affect lesion enhancement in the regression models ($P = .80$ and $P = .60$, respectively).

All cases of pure DCIS ($n = 5$) were detected as calcifications at mammography and were enhanced by an average of 59.6 HU ± 2.8, which was significantly greater than mean benign lesion enhancement ($P < .01$). The mean enhancements for invasive ductal carcinoma ($n = 10$), invasive mammary carcinoma ($n = 7$), mixed (invasive ductal carcinoma and DCIS or invasive mammary carcinoma and DCIS, $n = 6$), and mucinous ($n = 1$) cases were 47.3 HU ± 4.4, 57.3 HU ± 11.3, 71.3 HU ± 9.4, and 22.0 HU, respectively, none of which was significantly different from any other ($P = .12$). The single case of grade 2 mucinous adenocarcinoma showed a pattern of partial rim enhancement (Fig 4). All other malignant lesions showed homogeneous enhancement. In the subject with two fibroadenomas and a mixed invasive ductal carcinoma and DCIS lesion, the fibroadenomas enhanced by less than 20 HU, whereas the malignant mixed invasive ductal carcinoma and DCIS lesion enhanced by 112.5 HU, an almost sixfold difference.

Table 4

Regression-estimated Conspicuity Comparing Contrast-enhanced Breast CT with Unenhanced Breast CT

Parameter	Overall Mean	Mass Mean	Calcification Mean	Absolute Difference*
Overall	…	−1.20 (37)	−1.50 (17)	0.30 ($P = .34$)
Benign	−0.83 (25)	−0.69 (15)	−0.98 (10)	0.29 ($P = .46$)
Malignant	−1.71 (29)	−1.52 (22)	−2.37 (7)	0.85 ($P = .33$)
Absolute difference†	0.88 ($P < .001$)	0.83 ($P = .33$)	1.39 ($P = .01$)	0.56 ($P = .33$)‡

Note.—Unless otherwise indicated, data in parentheses are numbers of lesions. *P* values represent the significance of the difference in mixed-effects linear regression–estimated mean conspicuity scores for the compared lesion subgroups and have been adjusted for interradiologist variation, within-subject clustering, and breast density.

* Mass versus calcification.

† Benign versus malignant.

‡ Interaction of the malignancy and lesion type (mass or calcification) factors.

Figure 1

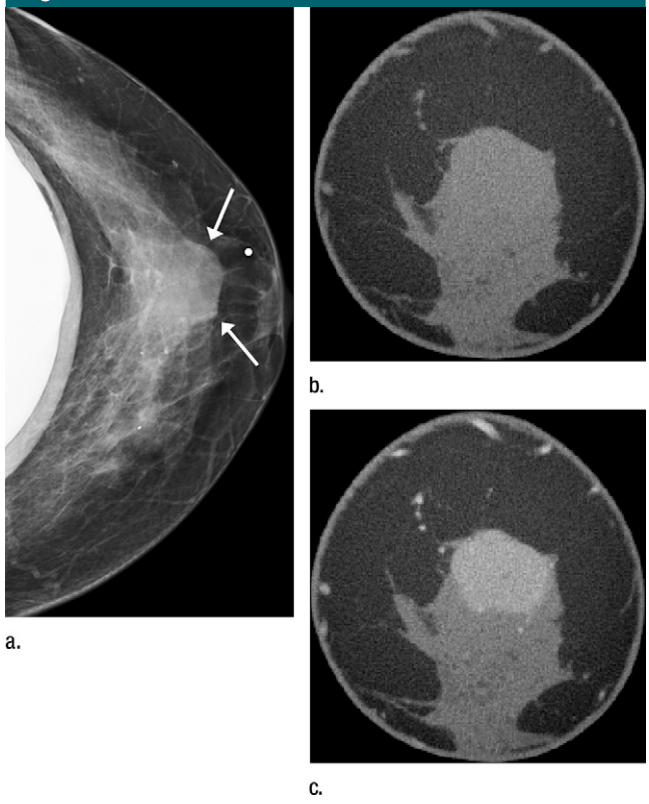

Figure 1: Images obtained in a 48-year-old woman. **(a)** Implant-displaced craniocaudal mammogram shows a mostly obscured mass (arrows). **(b)** Pre- and **(c)** postcontrast coronal breast CT images show the same invasive mammary carcinoma mass that enhanced 76.5 HU.

Discussion

Conspicuity of malignant breast masses at contrast-enhanced breast CT is significantly better than that at mammography or unenhanced breast CT, whereas conspicuity of malignant calcifications is better at contrast-enhanced breast CT than at unenhanced breast CT and is similar at contrast-enhanced breast CT and mammography. Malignant lesions have significantly greater conspicuity than do benign lesions at contrast-enhanced breast CT, possibly

Figure 2

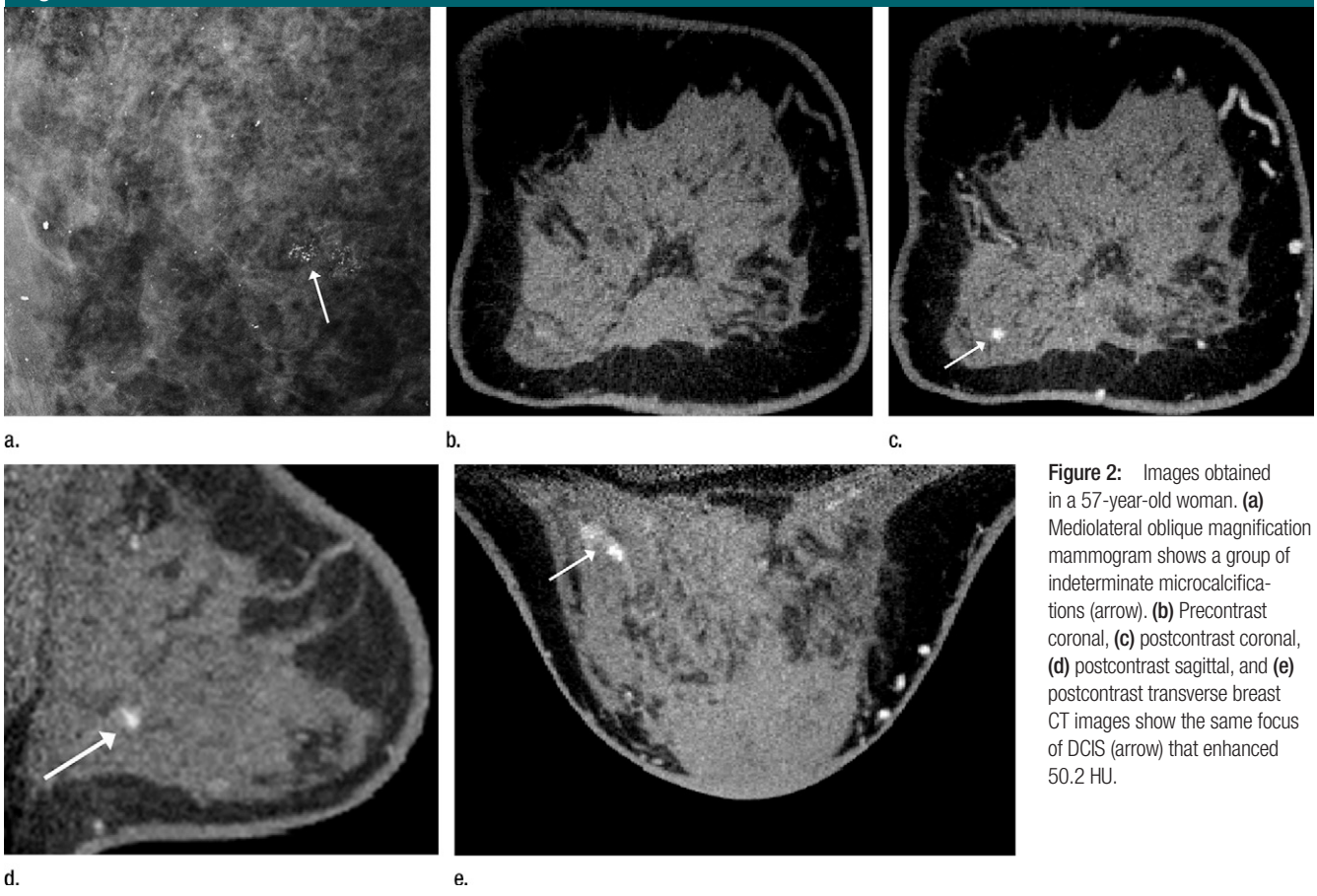

Figure 2: Images obtained in a 57-year-old woman. **(a)** Mediolateral oblique magnification mammogram shows a group of indeterminate microcalcifications (arrow). **(b)** Precontrast coronal, **(c)** postcontrast coronal, **(d)** postcontrast sagittal, and **(e)** postcontrast transverse breast CT images show the same focus of DCIS (arrow) that enhanced 50.2 HU.

Figure 3

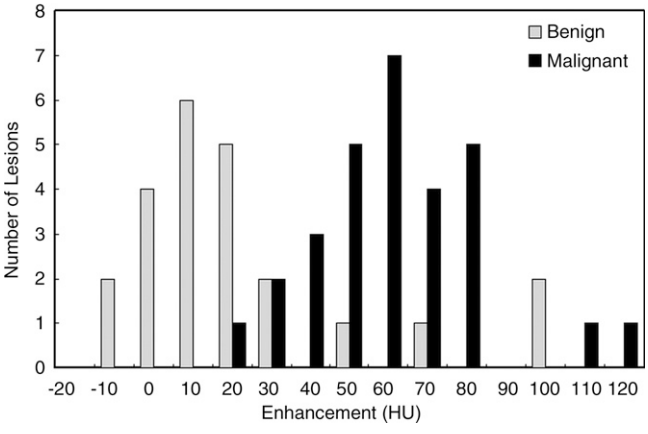

Figure 3: Bar graph shows enhancement of benign and malignant breast lesions.

improving the specificity of contrast-enhanced breast CT. In addition, the conspicuity of DCIS at contrast-enhanced breast CT is significantly greater than that at unenhanced breast CT and is similar to that at mammography.

Results of previous work showed that malignant calcifications were seen poorly with unenhanced breast CT when compared with malignant calcifications seen with mammography (2). Our results suggest that administration of contrast material may address this issue because the conspicuity of malignant calcifications at contrast-enhanced breast CT was significantly greater than that at unenhanced breast CT and similar to that at mammography. The conspicuity of benign calcifications continues to be significantly greater at mammography than at contrast-enhanced breast CT; however, this difference may be advantageous, possibly increasing the specificity of contrast-enhanced breast CT compared with that of mammography for DCIS.

Contrast-enhanced breast CT offers a promising quantitative technique with which to predict malignancy in breast lesions. Malignant lesions enhanced by

Radiology

Table 5

Regression-estimated Mean Enhancement at Contrast-enhanced Breast CT for Lesion Subgroups

Parameter	Overall Mean	Mass Mean	Calcification Mean	Absolute Difference*
Overall	…	38.0 (36)	40.4 (16)	2.4 ($P = .80$)
Benign	17.0 (23)	11.8 (14)	25.3 (9)	13.5 ($P = .22$)
Malignant	55.9 (29)	54.7 (22)	59.9 (7)	5.2 ($P = .6$)
Absolute difference†	38.9 ($P < .001$)	42.9 ($P < .001$)	34.6 ($P = .01$)	8.3 ($P = .6$)‡

Note.—Unless otherwise indicated, data in parentheses are numbers of lesions. *P* values represent the significance of the difference in mixed-effects linear regression–estimated mean enhancement for the compared lesion subgroups and have been adjusted for interradiologist variation, within-subject clustering, and breast density.

* Mass versus calcification.

† Benign versus malignant.

‡ Interaction of the malignancy and lesion type (mass or calcification) factors.

Figure 4

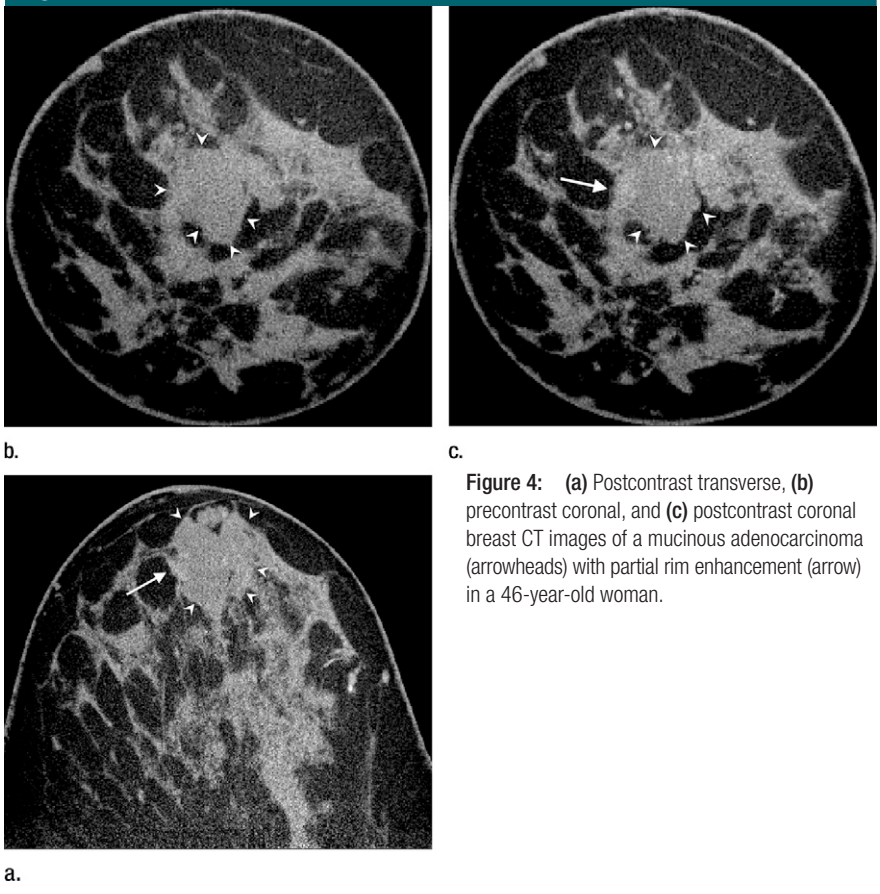

Figure 4: **(a)** Postcontrast transverse, **(b)** precontrast coronal, and **(c)** postcontrast coronal breast CT images of a mucinous adenocarcinoma (arrowheads) with partial rim enhancement (arrow) in a 46-year-old woman.

a mean of 38 HU more than did benign lesions ($P < .001$). Specifically, malignant calcifications enhanced by an average of 59.9 HU ± 2.0, with enhancement of DCIS lesions being significantly greater than that of benign lesions ($P < .01$). These quantitative findings also suggest improved specificity for contrast-enhanced breast CT in the detection of malignant calcifications.

The area under the receiver operating characteristic curve (0.876) shows the potential usefulness of quantitative enhancement of breast lesions in predicting malignancy. When combined with qualitative features, such as distribution, morphology, and margins, quantitative enhancement may be useful in predicting the malignant potential of an identified lesion. The area under the receiver operating characteristic curve reported in this study represents the predictive nature of only one quantitative measurement. We expect that with the addition of other morphologic information, the area under the receiver operating characteristic curve would increase. There also may be potential for the combination of quantified peak lesion enhancement at contrast-enhanced breast CT with other morphologic characteristics for the development of computer-aided diagnosis systems to improve diagnostic sensitivity and specificity.

The case of mucinous adenocarcinoma in this study emphasizes the importance of the enhancement pattern at contrast-enhanced breast CT and stresses the use of enhancement quantification only as an adjunct to qualitative assessment (17,18). This lesion showed a pattern of partial rim enhancement with a mean enhancement of 22.0 HU. At quantitative analysis, the hyperintense rim voxels were largely negated by the vast number of unenhanced voxels. Lesions with heterogeneous enhancement may require a more detailed voxel-by-voxel quantification technique, although the lesion morphology may be more valuable from a diagnostic standpoint.

Dynamic enhancement kinetics are used in lesion assessment in MR imaging, and generally three to seven data points are obtained. With contrast-enhanced breast CT, only one time point of enhancement is shown. The value of the kinetic curve in dynamic contrast-enhanced MR imaging remains unclear. Results from a multicenter study of diagnostic features at dynamic contrast-enhanced MR imaging suggested that margin features and qualitative early-phase enhancement intensity are the most important features in the classification of breast masses

(19). Morphologic information gained from high-spatial-resolution imaging is more diagnostically valuable than the kinetic information lost by sacrificing temporal resolution (20). The spatial resolution of breast CT is considerably greater than that of breast MR imaging. Typically, in breast MR imaging, both breasts are imaged with arrays of 256–512 pixels, which—for the field of view included (about 300–350 mm)—translates to MR imaging voxel dimensions of between 0.6 and 1.4 mm, with section thicknesses varying from 1 to 4 mm. Voxel dimensions at breast CT are about 0.25 mm. Thus, the voxel volumes at breast CT are on the order of 20–500 times smaller than those at breast MR imaging.

Dedicated breast CT may, however, be able to help assess contrast material enhancement kinetics, and a variety of techniques are being explored for this purpose. These include the use of dual-energy subtraction images acquired with the breast CT system in a stationary mode, with high temporal resolution and low radiation dose to the breast. Alternatively, a continuous slip-ring CT acquisition scheme in which minimal views and real-time iterative reconstruction techniques are used may yield a low-radiation-dose technique for rough enhancement kinetic assessment on fully tomographic images.

Our study had limitations. The assessment of conspicuity between modalities was subjective and led to potential bias, since the readers knew the types of modalities that were being compared. Two of the radiologists involved in subject recruitment evaluated the images in sequential order, which possibly led to recall bias. Subjects were selected for breast CT studies on the basis of the results of standard breast imaging studies, which might have created a conspicuity bias toward mammography. There was significant interobserver variability in comparing contrast-enhanced breast CT with unenhanced breast CT ($P = .05$). This variability may have been attributable to a difference in observer familiarity with breast CT images because one observer (K.K.L.) had substantially more experience reading breast CT images. On average, the observer with less experience reported a larger conspicuity difference at contrast-enhanced breast CT than at unenhanced breast CT than did the observer with more experience. The number of lesions ($n = 54$) included in this pilot study was small. The number of malignant lesions with calcifications ($n = 7$) and, specifically, the number diagnosed as pure DCIS ($n = 5$) might not have been a representative sample. Randomized blinded multicenter trials with larger sample sizes are needed to characterize the detection rate, sensitivity, and specificity of contrast-enhanced breast CT versus the detection rate, sensitivity, and specificity of mammography.

The contrast material protocols used in this study were derived empirically. The optimal delay from injection to scanning and the optimal contrast material dose have yet to be determined. Subject body mass was not taken into account. Assuming iodinated contrast material kinetics are similar to the kinetics of gadolinium-based contrast agents, we may have used a suboptimal delay in this study and scanned patients before or after peak enhancement. Although regression models showed that delay did not affect lesion enhancement significantly, the differential enhancement between benign and malignant lesions measured in this study may lead to underestimation of the maximum attainable difference.

Quantification of lesion enhancement at contrast-enhanced breast CT shows potential to aid in the prediction of malignancy. Manual outlining was used to segment lesions from the breast and to quantify enhancement, but automated techniques would be required for use in a clinical setting.

One possible limitation to the current design of our dedicated breast CT scanner may be its ability to scan only one breast at a time. However, the importance of contrast material delay in lesion detection must be clarified before necessitating simultaneous imaging of both breasts. Future studies are necessary to determine whether bilateral dynamic contrast-enhanced breast CT is necessary to increase the specificity of the modality, as in MR imaging.

Despite these limitations, malignant lesions are more conspicuous at contrast-enhanced breast CT than at mammography or unenhanced breast CT. Contrast-enhanced breast CT may offer an alternative to dynamic contrast-enhanced MR imaging, particularly for cancer screening in women at high risk for breast cancer and for local staging in women with newly diagnosed breast cancer. Contrast-enhanced breast CT requires ionizing radiation; however, the imaging procedure is faster than the imaging procedure for dynamic contrast-enhanced MR imaging, and it is likely less expensive. With its open architecture, contrast-enhanced breast CT also may be better suited for patients who are claustrophobic or obese or who have other contraindications to dynamic contrast-enhanced MR imaging. Other breast CT systems with an expanded open architecture are under construction to further improve access to the breast, thereby enabling image-guided biopsy and delivery of therapy.

In summary, we have shown that malignant lesions are significantly more conspicuous at contrast-enhanced breast CT when compared with findings at unenhanced breast CT or mammography. The conspicuity of malignant calcifications is significantly improved compared with that of unenhanced breast CT and is not significantly different from the conspicuity of malignant calcifications at mammography. Quantification of lesion enhancement at contrast-enhanced breast CT likely will be helpful in improving both the sensitivity and the specificity of dedicated breast CT. Although more studies must be conducted to optimize contrast-enhanced breast CT protocols, our results suggest that contrast-enhanced breast CT is a promising modality with which to detect and diagnose breast cancer.

Acknowledgments: We thank Terry L. Coates, MD, Department of Radiology, University of California Davis Medical Center, for her assistance with subject recruitment and breast lesion conspicuity scoring and Yue-ju Li, MS, Department of Public Health Sciences, University of California Davis, for her statistical programming support.

References

1. American Cancer Society. Breast cancer facts and figures 2009-2010. Atlanta, Ga: American Cancer Society, 2010.
2. Lindfors KK, Boone JM, Nelson TR, Yang K, Kwan AL, Miller DF. Dedicated breast CT: initial clinical experience. Radiology 2008;246(3):725–733.
3. Newell D, Nie K, Chen JH, et al. Selection of diagnostic features on breast MRI to differentiate between malignant and benign lesions using computer-aided diagnosis: differences in lesions presenting as mass and non-mass-like enhancement. Eur Radiol 2010; 20(4):771–781.
4. Chen SC, Carton AK, Albert M, Conant EF, Schnall MD, Maidment AD. Initial clinical experience with contrast-enhanced digital breast tomosynthesis. Acad Radiol 2007; 14(2):229–238.
5. Perrone A, Lo Mele L, Sassi S, et al. MDCT of the breast. AJR Am J Roentgenol 2008; 190(6):1644–1651.
6. Jong RA, Yaffe MJ, Skarpathiotakis M, et al. Contrast-enhanced digital mammography: initial clinical experience. Radiology 2003;228(3):842–850.
7. Zhao H, Xu R, Ouyang Q, Chen L, Dong B, Huihua Y. Contrast-enhanced ultrasound is helpful in the differentiation of malignant and benign breast lesions. Eur J Radiol 2010;73(2):288–293.
8. Goh V, Padhani AR. Imaging tumor angiogenesis: functional assessment using MDCT or MRI? Abdom Imaging 2006;31(2):194–199.
9. Dawson P. Functional imaging in CT. Eur J Radiol 2006;60(3):331–340.
10. Miles KA. Tumour angiogenesis and its relation to contrast enhancement on computed tomography: a review. Eur J Radiol 1999;30(3):198–205.
11. Cuenod CA, Fournier L, Balvay D, Guinebretière JM. Tumor angiogenesis: pathophysiology and implications for contrast-enhanced MRI and CT assessment. Abdom Imaging 2006;31(2):188–193.
12. Chang CH, Sibala JL, Fritz SL, Dwyer SJ 3rd, Templeton AW. Specific value of computed tomographic breast scanner (CT/M) in diagnosis of breast diseases. Radiology 1979;132(3):647–652.
13. Chang CH, Sibala JL, Fritz SL, et al. Computed tomography in detection and diagnosis of breast cancer. Cancer 1980;46 (4 suppl):939–946.
14. Chang CH, Sibala JL, Fritz SL, Gallagher JH, Dwyer SJ 3rd, Templeton AW. Computed tomographic evaluation of the breast. AJR Am J Roentgenol 1978;131(3):459–464.
15. Boone JM, Kwan AL, Yang K, Burkett GW, Lindfors KK, Nelson TR. Computed tomography for imaging the breast. J Mammary Gland Biol Neoplasia 2006;11(2):103–111.
16. Boone JM, Kwan AL, Seibert JA, Shah N, Lindfors KK, Nelson TR. Technique factors and their relationship to radiation dose in pendant geometry breast CT. Med Phys 2005;32(12):3767–3776.
17. Okafuji T, Yabuuchi H, Soeda H, et al. Circumscribed mass lesions on mammography: dynamic contrast-enhanced MR imaging to differentiate malignancy and benignancy. Magn Reson Med Sci 2008;7(4):195–204.
18. Inoue M, Sano T, Watai R, et al. Dynamic multidetector CT of breast tumors: diagnostic features and comparison with conventional techniques. AJR Am J Roentgenol 2003;181(3):679–686.
19. Schnall MD, Blume J, Bluemke DA, et al. Diagnostic architectural and dynamic features at breast MR imaging: multicenter study. Radiology 2006;238(1):42–53.
20. Kuhl CK, Schild HH, Morakkabati N. Dynamic bilateral contrast-enhanced MR imaging of the breast: trade-off between spatial and temporal resolution. Radiology 2005; 236(3):789–800.